

The grouping, merging and survival of subhaloes in the simulated Local Group

Jarosław Klimentowski,¹ Ewa L. Łokas,¹ Alexander Knebe,² Stefan Gottlöber,³ Luis A. Martinez-Vaquero,² Gustavo Yepes² and Yehuda Hoffman⁴

¹*Nicolaus Copernicus Astronomical Center, Bartycka 18, 00-716 Warsaw, Poland*

²*Grupo de Astrofísica, Departamento de Física Teórica, Modulo C-XI, Facultad de Ciencias, Universidad Autónoma de Madrid, 28049 Cantoblanco, Madrid, Spain*

³*Astrophysikalisches Institut Potsdam, An der Sternwarte 16, 14482 Potsdam, Germany*

⁴*Racah Institute of Physics, Hebrew University, Jerusalem 91904, Israel*

31 October 2018

ABSTRACT

We use a simulation performed within the Constrained Local UniversE Simulation (CLUES) project to study a realistic Local Group-like object. We employ this group as a numerical laboratory for studying the evolution of the population of its subhaloes from the point of view of the effects it may have on the origin of different types of dwarf galaxies. We focus on the processes of tidal stripping of the satellites, their interaction, merging and grouping before infall. The tidal stripping manifests itself in the transition between the phase of mass accretion and mass loss seen in most subhaloes, which occurs at the moment of infall on to the host halo, and the change of the shape of their mass function with redshift. Although the satellites often form groups, they are loosely bound within them and do not interact with each other. The infall of a large group could however explain the observed peculiar distribution of the Local Group satellites, but only if it occurred recently. Mergers between prospective subhaloes are significant only during an early stage of evolution, i.e. more than 7 Gyr ago, when they are still outside the host haloes. Such events could thus contribute to the formation of more distant early type Milky Way companions. Once the subhaloes enter the host halo the mergers become very rare.

Key words: methods: N -body simulations – galaxies: Local Group – galaxies: dwarf – galaxies: fundamental parameters – galaxies: kinematics and dynamics – cosmology: dark matter

1 INTRODUCTION

According to the favoured Λ CDM model galaxies are formed in a hierarchical way (White & Rees 1978). Small galaxies form first and then merge into larger structures. In this scenario the surviving dwarf galaxies can be viewed as tracers of the early Universe. Understanding their properties and evolution is crucial to understanding the Λ CDM Universe itself.

The Local Group (LG) is the closest and best studied object of the extragalactic scale (see van den Bergh 1999 for a review). Apart from the two large spirals, the Milky Way (MW) and Andromeda (M31), it is populated by several tens of dwarf galaxies which by their morphological properties can be divided into irregulars, ellipticals and spheroidals (Mateo 1998). They are known as the classical dwarfs. Recently we have witnessed many new discoveries of ultra faint satellite galaxies in the halo of the MW (e.g.

Sakamoto & Hasegawa 2006; Zucker et al. 2006; Belokurov et al. 2008). The dynamical properties of these objects are still very poorly studied, but their alleged extremely high mass to light ratios (Simon & Geha 2007) suggest that they might be a rather different class of objects.

One could expect that an early Universe progenitor of a dwarf galaxy should be similar for all types of the present classical dwarfs (Kravtsov, Gnedin & Klypin 2004) and would consist of a dark matter halo of mass around $10^9 M_{\odot}$. This amount of mass would allow it to accrete gas even in the highly ionized environment of the early Universe. The conservation of angular momentum would require that the gas and the stellar component formed a disk rather than a spheroid. Such an object would then undergo evolution due to baryonic processes such as cooling, star formation, supernova feedback, photoevaporation of the gas and heating by the cosmic ultraviolet background. It remains to be seen if

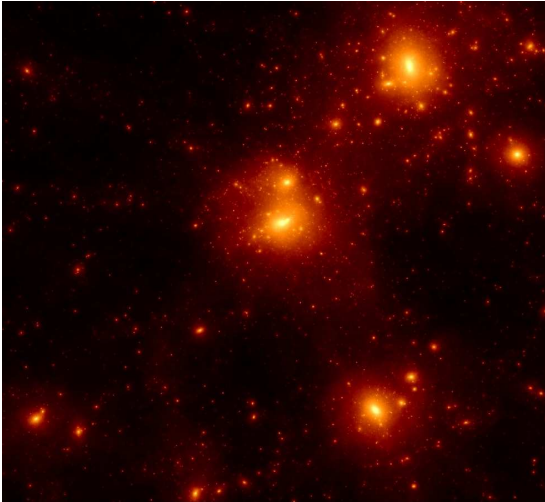


Figure 1. Overview of the simulated LG. M31 is located in the centre of the image, MW at the top right. The image size is $3 h^{-1}\text{Mpc}$.

these or rather the environmental, purely gravitational processes were the dominant factor in shaping dwarf galaxies. In this work we focus on the latter which can be modelled with simulations following only the dark matter component.

The studies of stellar populations and kinematics of dwarf galaxies provide some general hints (see Tolstoy, Hill & Tosi 2009 for a recent review) concerning the possible environmental effects. The late type dwarfs (dwarf irregulars) possess rich star formation histories, high amounts of hydrogen in stellar disks and significant angular momenta. They are usually isolated objects (except for the Magellanic Clouds). These facts suggest that they evolved in isolation only by the internal baryonic processes. On the other hand, the early type dwarfs usually lack gas and do not show any signs of recent star formation. They also possess very low or no angular momentum. They typically are close companions to the MW and M31, but even those isolated ones like Tucana or Cetus could have evolved in the vicinity of the large spirals and been ejected recently to more distant orbits (Gill, Knebe & Gibson 2005; Sales et al. 2007a; Ludlow et al. 2009). They have high mass-to-light ratios from about ten to a few hundred solar units. They could have evolved from a disk like those present in dwarf irregulars by strong gravitational interactions. These interactions could take the form of mergers or tidal forces.

The latter idea has been developed into the so-called tidal stirring scenario (Mayer et al. 2001). Using N-body simulations it has been demonstrated that indeed a transformation from a disk to the dwarf spheroidal is possible by pure tidal interactions with a host galaxy. Mayer et al. (2001) have shown that low surface brightness disks would produce dwarf spheroidal galaxies we observe today, while high surface brightness disks would lead to the formation of dwarf ellipticals. Depending on the adopted star formation history this scenario is able to reproduce dwarf spheroidals with moderate mass-to-light ratios (Klimentowski et al. 2007, 2009) as well as strongly dark matter dominated ones if the gas is expelled early on (Mayer et al. 2007).

Mergers and interactions between dwarfs could be an-

Table 1. The properties of the LG: distance and relative velocity between the two main members, the velocity dispersion around the Hubble flow, the overdensity within a sphere of 7 Mpc centred on the LG, distance from the LG to the Virgo cluster and the virgocentric flow. The second column gives the values from the simulation. For comparison, the third column provides also the observed values. The references for the observed values in the last column are: 1 - Karachentsev et al. (2004); 2 - van der Marel & Guhathakurta (2008); 3 - Tikhonov & Klypin (2009); 4 - Hudson (1993); 5 - Fouqué et al. (2001); 6 - Tonry et al. (2000).

Property	Simulated	Observed	Ref.
d (M31–MW)	$0.91 h^{-1} \text{ Mpc}$	0.77 Mpc	1
V_{rel} (M31–MW)	-193 km s^{-1}	-130 km s^{-1}	2
$\sigma_{\text{H}}(r < 7 \text{ Mpc})$	100 km s^{-1}	90 km s^{-1}	3
$\delta\rho/\bar{\rho}(r < 7 \text{ Mpc})$	0.82	0.8	4
d (LG–Virgo)	$10.9 h^{-1} \text{ Mpc}$	18.0 Mpc	5
Virgocentric flow	-255 km s^{-1}	-409 km s^{-1}	6

other channel for the formation of early type dwarfs since they could lead to a very strong evolution (e.g. Knebe et al. 2006; Angulo et al. 2009), as in the case of larger galaxies (e.g. Springel, Di Matteo & Hernquist 2005). It has also recently been proposed that dwarf galaxies might be accreted on to their hosts in groups which may explain e.g. the particular distribution of dwarfs around the MW and M31 (Libeskind et al. 2005; Metz, Kroupa & Jerjen 2007, 2009a; D’Onghia & Lake 2008; Li & Helmi 2008; Metz et al. 2009b). In this work we discuss this second scenario of the formation of early type dwarf galaxies using a cosmological N -body simulation of a LG. Our purpose is to study mergers and interactions of haloes which end up as subhaloes. We also consider the infall of these objects together as a group of small haloes.

The paper is organized as follows. Section 2 contains the description of the simulation used in this analysis and the halo finding algorithm which provides the basis for this study. In section 3 we characterize the main properties of the subhalo population of the two largest haloes; we discuss their mass functions, their survival times and the evolution of their masses. In section 4 we study the behaviour of subhaloes in groups; we provide the statistics of groups around the two largest haloes, describe the mass functions of the largest groups and follow their history. The effect of mergers and interactions between subhaloes is discussed in section 5. The discussion follows in section 6.

2 THE SIMULATION

We analyze a constrained dark matter simulation of the LG. This simulation is part of the CLUES project¹, a collaboration whose main goal is to produce realistic cosmological simulations of the Local Universe by imposing observational constraints on the mass and velocity fields of the initial random Gaussian fluctuation realizations. For this simulation we have used a box of $64h^{-1}\text{Mpc}$ size assuming a spatially flat cosmological model with WMAP3 parameters (Spergel

¹ <http://clues-project.org>

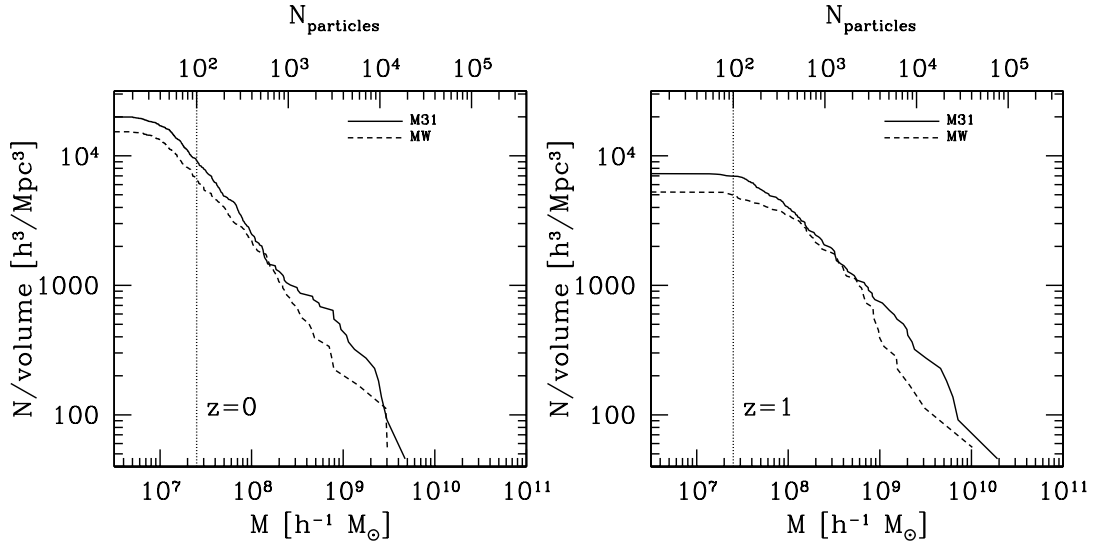


Figure 2. The cumulative mass function of subhaloes found within one virial radius of two most massive haloes normalized by the volume of that region. The left panel shows $N(> M)$ at redshift $z = 0$. The right panel presents the mass function of the same haloes traced back to redshift $z = 1$. The upper axis indicates the number of particles in a halo. Vertical dotted lines indicate our completeness limit of 100 particles.

Table 2. The properties of the five most massive haloes identified in the simulation. The columns list the assigned name of a halo, its virial mass, the virial radius, the number of particles inside the virial radius and the spin parameter (according to Peebles definition).

Name	$M_{\text{vir}} [10^{11} h^{-1} M_{\odot}]$	$r_{\text{vir}} [h^{-1} \text{kpc}]$	N	λ
Andromeda (M31)	5.69	173.5	2239732	0.0686
Milky Way (MW)	4.62	162.0	1821419	0.0607
3rd halo	2.66	134.7	1045831	0.0722
4th halo	2.24	127.2	883066	0.0219
5th halo	2.01	122.7	738875	0.0420

et al. 2007): $\Omega_m = 0.24$, $\Omega_b = 0.042$, $\Omega_{\Lambda} = 0.76$, the Hubble constant $h = 0.73$, the normalization $\sigma_8 = 0.75$ and the slope $n = 0.95$ of the power spectrum.

First, a constrained density field on a grid of 256^3 mesh points was obtained applying the Hoffman & Ribak (1991) algorithm for generating constrained realizations of Gaussian random fields. As observational constraints we have used the radial velocities of galaxies drawn from the MARK III catalogue (Willick et al. 1997), Surface Brightness Fluctuation survey (Tonry et al. 2001) and the local volume galaxy catalog (Karachentsev et al. 2004) as well as the positions of nearby X-ray selected clusters of galaxies (Reiprich & Böhringer 2002). The algorithm has been described in detail in Zaroubi, Hoffman & Dekel (1999), Kravtsov, Klypin & Hoffman (2002) and Klypin et al. (2003). With this algorithm to calculate the initial conditions the resulting simulation contains the main features which characterize the Local Universe. In the large simulation box the Virgo as well as the Coma cluster and the Great Attractor are approximately at the right positions whereas the small scale structure is essentially random. A smaller box like the one we discuss here contains an object which can be identified as the Virgo cluster.

Within our simulation box we represent the linear power spectrum at redshift $z = 100$ by $N_{\text{max}} = 4096^3$ particles of mass $m_{\text{DM}} = 2.5 \times 10^5 h^{-1} M_{\odot}$. We then Fourier transform

the constrained density field and substitute the overlapping Fourier modes in our otherwise random realization. At first we degrade the mass resolution to 256^3 particles and identify the position of the simulated LG at $z = 0$. To this end we start at the position of the simulated Virgo cluster and search for a Local Group like object at the right position. After identifying such an object we find all the particles within a sphere of radius $2h^{-1} \text{Mpc}$ centred on the simulated object and determine the Lagrangian coordinates of these particles in the initial conditions.

In a next step we resimulate the evolution of the LG using the full resolution (4096^3) within this sphere of radius $2h^{-1} \text{Mpc}$. Here we follow the algorithm described in Klypin et al. (2001) and degrade the mass and force resolution in those areas that are far away from the Lagrangian region from which the LG forms. To this end we put concentric regions around the high-resolution area, each of them populated with particles 8 times more massive. In the end we have five different mass refinements ranging from 4096^3 at the high resolution area to 256^3 in the outer parts of the simulation box. Thus we simulate with very high resolution the evolution of the LG in the right environment. The evolution of the same region has been also simulated including gas dynamics and star formation (Libeskind et al. 2009).

The simulation has been performed using the TreePM parallel N -body code GADGET2 (Springel 2005). For the

high mass resolution particles we used a fixed comoving Plummer equivalent softening of $500 h^{-1}$ pc at early redshift and changed to $100 h^{-1}$ pc physical since $z = 4$. For the rest of the mass refinement levels, we increase the Plummer softening by a factor of approximately two at every level. To follow the evolution of the LG we have stored in total 134 outputs equally spaced in time, which translates into a time difference of 0.1 Gyr between consecutive snapshots. The overview of the simulated LG in the final output is shown in Fig. 1 and its properties are listed in Table 1. The properties of its five most massive haloes are given in Table 2.

In order to identify haloes and subhaloes in our simulation we have run the MPI+OpenMP hybrid halo finder AHF (AMIGA halo finder, to be downloaded freely from <http://www.popia.ft.uam.es/AMIGA>). AHF is an improved version of the MHF halo finder (Gill, Knebe & Gibson 2004a), which locates local overdensities in an adaptively smoothed density field as prospective halo centres. The local potential minima are computed for each of these density peaks and the gravitationally bound particles are determined. We stress that our halo finding algorithm automatically identifies haloes, subhaloes, subsubhaloes, etc. For more details on the mode of operation and the actual functionality we refer the reader to Knollmann & Knebe (2009) where the AHF halo finder is described in detail.

For each halo, we compute the virial radius r_{vir} at which the density $M(< r)/(4\pi r^3/3)$ drops below $\Delta_{\text{vir}}\rho_{\text{b}}$ where ρ_{b} is the cosmological background density. The threshold Δ_{vir} is computed using the spherical top-hat collapse model and is a function of both cosmological model and time (e.g. Lokas & Hoffman 2001). For the cosmology we are using, $\Delta_{\text{vir}} = 355$ at $z = 0$. Subhaloes are defined as haloes which lie within the virial region of a more massive halo, the so-called host halo. As subhaloes are embedded within the density of their respective host halo their very own density profile usually shows a characteristic upturn at a radius $r_{\text{t}} \lesssim r_{\text{vir}}$, where r_{vir} would be their actual (virial) radius if they were found in isolation.² We use this ‘truncation radius’ r_{t} as the outer edge of the subhalo and hence (sub)halo properties (i.e. mass, density profile, velocity dispersion, rotation curve) are calculated using the gravitationally bound particles inside either the virial radius r_{vir} for a host halo or the truncation radius r_{t} for a subhalo.

Once the halo finding is completed all haloes are traced back in time. For this purpose the halo must be linked to its progenitor in the previous simulation output. We do that using the following prescription. A halo progenitor is identified in the previous snapshot by maximizing the ratio $C_i^2/(N_i N_j)$, where C_i is the number of common particles shared between the i -th halo of the current snapshot and the j -th halo of the previous snapshot while N_i and N_j are the total numbers of particles in these haloes.

This simple formula works surprisingly well in identifying the correct halo in the past. Unfortunately, sometimes the correct halo is missing in the previous snapshot because

² Note that the actual density profile of subhaloes after the removal of the host’s background drops faster than for isolated haloes (e.g. Kazantzidis et al. 2004a); only when measured within the background still present we will find the characteristic upturn used here to define the truncation radius r_{t} .

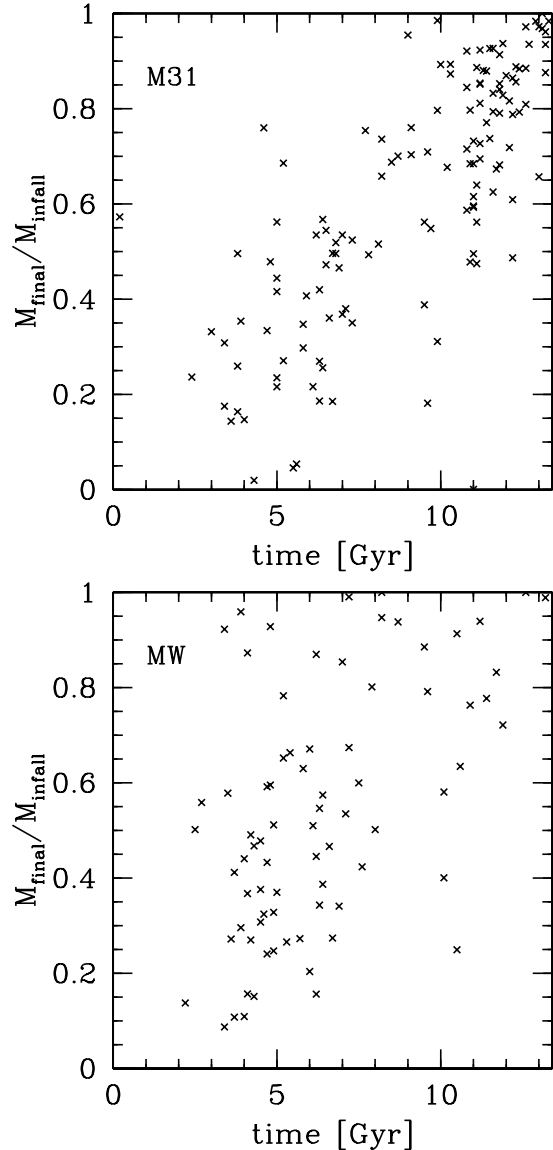


Figure 3. The ratio between the final mass of a subhalo at the end of the simulation and its mass at the infall time, as a function of infall time for M31 (upper panel) and MW (lower panel).

it was not found by the halo finder. This happens, for example, when a smaller halo passes close to the centre of a larger one and due to its low density contrast the halo finder may not be able to identify it. To take care of this problem (wrong identification would lead to something which looks like a halo splitting in two) we also check that the mass of the progenitor is close to the mass of the descendant: if the mass ratio is smaller than 0.8 we look for the correct progenitor halo two (instead of one) snapshots earlier. This parameter was tuned to the actual properties of the halo finder. This procedure is applied recursively until we find a credible progenitor in one of the higher redshift snapshots. In practice, however, we never have to skip more than one or two snapshots.

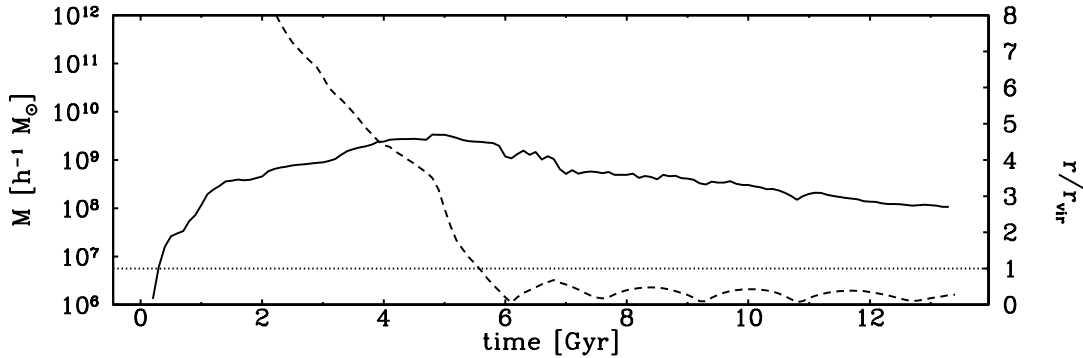


Figure 4. Example of the evolution of a satellite subhalo. The solid line shows the mass of the subhalo and the dashed one its distance from the host galaxy divided by its evolving virial radius, as a function of time. The dotted line shows the distance of one virial radius from the host, which we adopt as a measure of the orbit entry point for the subhalo. During the first stage of the evolution the subhalo gains mass. After entering the orbit around its host it starts losing mass due to tidal stripping.

3 PROPERTIES OF THE SATELLITES

The first two rows of Table 2 list the properties of the two most massive haloes identified in the last simulation output corresponding to redshift $z = 0$. We will call the largest one Andromeda (M31) and the second largest the Milky Way (MW). In this section we study in detail the properties of the satellites of these largest haloes. The left panel of Fig. 2 shows the mass function $N(> M)$ of all subhaloes belonging to the two most massive haloes at redshift $z = 0$. The subhaloes were identified within one virial radius of their host. The relation was scaled by the volume of each region in which subhaloes were selected. In this case the mass functions are very similar for both haloes. Note that the shapes of the mass functions flatten towards smaller masses signifying loss of completeness. This happens at masses corresponding to about 100 bound particles or $2.5 \times 10^7 h^{-1} M_{\odot}$. Unless otherwise stated, from now on we will consider only haloes with masses above this value.

The right panel of Fig. 2 shows the cumulative mass function of all subhaloes found at redshift $z = 0$ traced back to $z = 1$. Comparing the panels we see that with decreasing redshift the number density of small mass haloes increases and the whole slope of the relation steepens. This suggests that subhaloes which were originally more massive lose mass during their evolution. This process is due to the tidal interactions of subhaloes with their host halo and is common for satellites of all large galaxies (cf. Mayer et al. 2001; Gill et al. 2004b; Giocoli, Tormen & van den Bosch 2008).

This phenomenon is further illustrated in Fig. 3 which shows the ratio between the final mass of a surviving satellite at the end of the simulation and its mass at the infall or orbit entry time as a function of infall time, i.e. the time it crosses the virial radius of the host for the first time. The tendency for mass loss is clearly seen as the ratios are typically much lower than one especially for those haloes which became satellites early. Figure 4 shows this process in detail for a single example subhalo. During its evolution it first gains mass as the hierarchical formation scenario predicts, but then reaches a point at which it starts losing mass. As expected, the moment when the mass trend reverses is close to the time at which the subhalo becomes a satellite of a larger halo, which will be its host for the rest of the simula-

tion. From that moment on the satellite is being stripped by tidal forces of the host. The mass loss obviously depends on the infall time but also on other parameters like the orbit. The presented example is a rather extreme case. According to Fig. 3 most haloes do not lose that much mass. Also not all subhaloes follow this path of evolution. Many of them just fall into the host halo and merge with it.

Figure 5 shows the survival time of a satellite in terms of the number of pericentre passages it sustains. In the upper panel only those satellites were selected which *did not* survive until the end of the simulation and were completely destroyed. Many subhaloes do not survive even a single pericentre passage, they fall straight inside and merge with the host. This behaviour is in agreement with other N -body studies where it was found that majority of stars in the present MW halo comes from the most massive subhaloes that were accreted in the past (e.g. Bullock & Johnston 2005; Sales et al. 2007b). There are however still more than a hundred of satellites per halo, which were able to survive up to eight pericentre passages. Their orbital history is illustrated by the histogram in the lower panel of Fig. 5. Presumably, these might be the dwarf spheroidal galaxies of the LG that we presently see as, according to the tidal stirring scenario (Mayer et al. 2001; Klimentowski et al. 2009), a significant number of pericentric passages accompanied by substantial mass loss are required to transform a disk stellar component into a spheroid.

Actually, at the end of the simulation, M31 has 198 and the MW 136 surviving subhaloes inside the virial radius. It is interesting to look at the distribution of the shapes of the orbits of these subhaloes. Figure 6 plots the apocentre versus pericentre (r_a and r_p) for those subhaloes that survived until the end and completed at least one orbit around their host. Note that M31 subhaloes are strongly underrepresented because many of them found inside the virial radius at the end have not yet completed a single orbit (see the next section). Figure 7 presents the distribution of the ratio r_p/r_a of the same subhaloes. We can see that there is a strong preference for rather eccentric orbits in agreement with the results found by Gill et al. (2004b) and Diemand, Kuhlen & Madau (2007).

Figure 8 shows the mass of subhaloes at the moment of orbit entry as a function of redshift at which the infall of

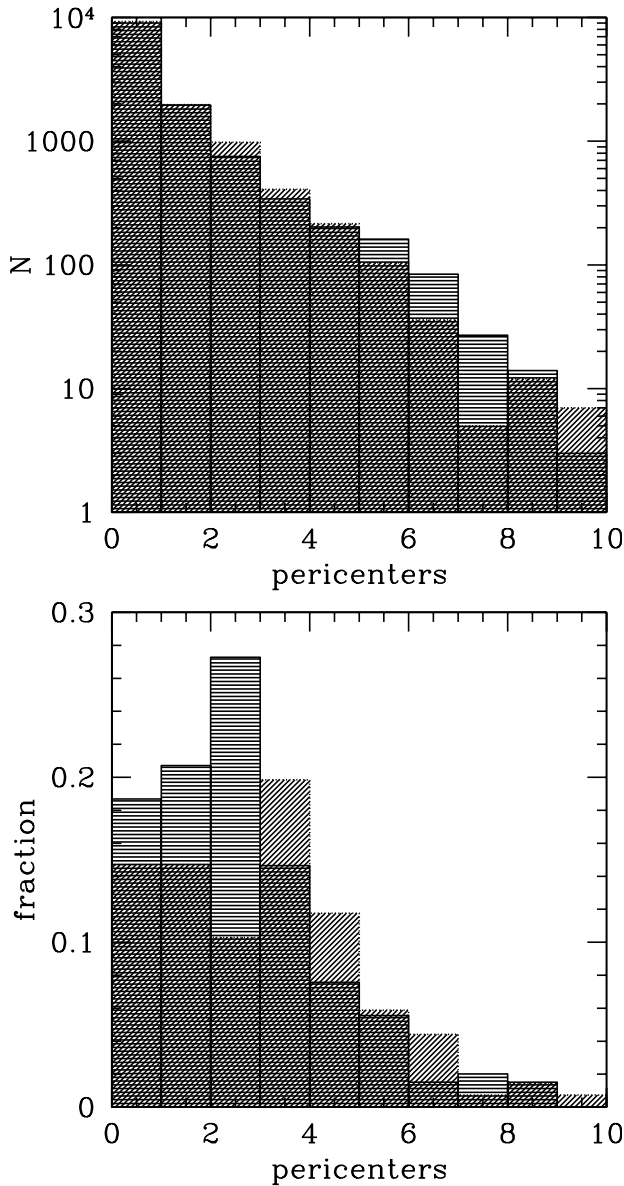


Figure 5. The survival of subhaloes. The upper panel shows the numbers of pericentre passages survived by subhaloes before their destruction therefore it shows those which eventually *did not* survive until the present. Subhaloes with zero pericentre passages were accreted directly on to the host halo and destroyed during their first passage. The lower panel corresponds to those subhaloes which survived until the end of the simulation and shows the fraction of subhaloes that survived a given number of pericentre passages to all surviving subhaloes separately in the M31 and in the MW. Here subhaloes with zero pericentre passages have entered their host recently and have not yet reached the pericentre of their orbit. In each panel the horizontal shading corresponds to the M31, the skewed one to the MW.

the subhalo takes place. The Figure allows us to hypothesize on the possible evolution of the subhaloes in different mass ranges. The majority of large mass subhaloes (with masses around $10^9 M_{\odot}$) enter their orbits at around $z = 1$. These are most probably the progenitors of dwarf spheroidal galaxies. As shown in Klimentowski et. al (2009) a halo of this mass possessing a stellar disk at $z = 1$ has enough time

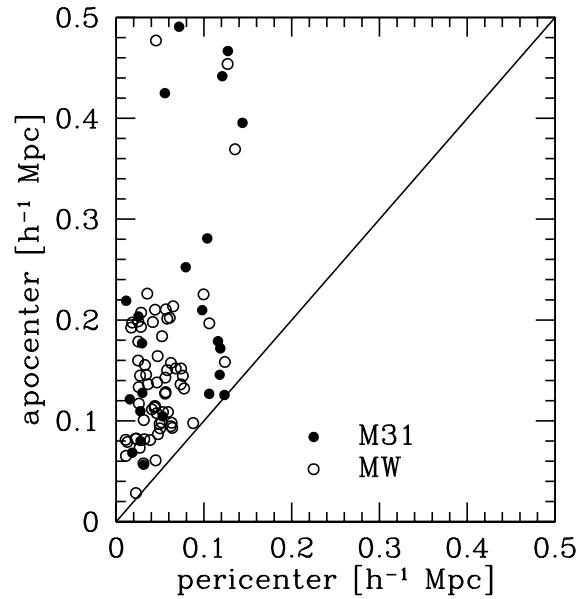


Figure 6. The distribution of orbits for subhaloes that survived until the present, were found inside the virial radius of the host and completed at least one orbit around it. The filled and open circles show the apocentre versus pericentre distance respectively for M31 and MW subhaloes. The line indicates the circular orbits.

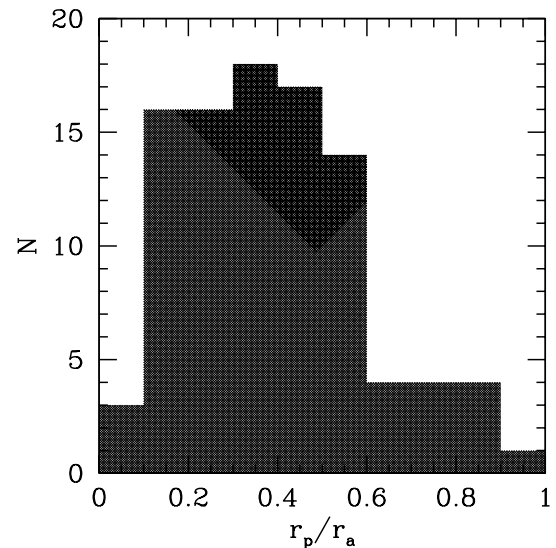


Figure 7. The distribution of peri- to apocentre ratio for the same sample of M31 and MW subhaloes as shown in Fig. 6.

to form a dwarf spheroidal by the present by tidal stirring. The mass loss that occurs in this process can be very significant as demonstrated by Fig. 3 (cf. Mayer et al. 2001; Hayashi et al. 2003; Gill et al. 2004b; Kazantzidis, Moore & Mayer 2004b; Kampakoglou & Benson 2007; Klimentowski et al. 2007, 2009; Peñarrubia, Navarro & McConnachie 2008; Giocoli et al. 2008) which at the end of the evolution leaves us with masses of the order of few times $10^7 M_{\odot}$, as indeed measured for most dwarf spheroidals (e.g. Lokas et al. 2008; Lokas 2009).

The subhaloes that start orbiting their host later most probably correspond to dwarf irregular galaxies, as they al-

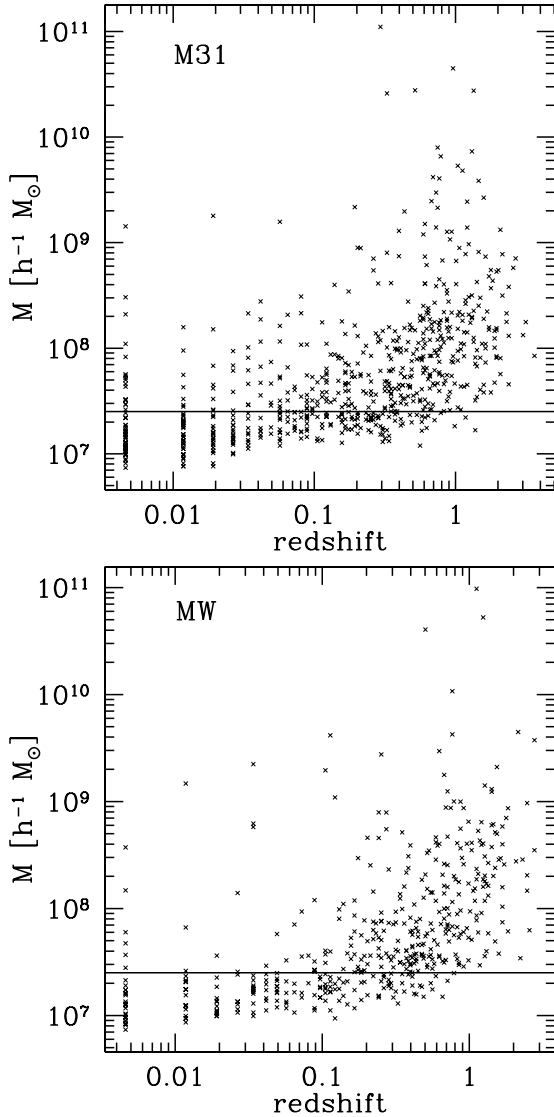


Figure 8. The maximum mass of a subhalo as a function of redshift at which this mass was reached. The mass corresponds to the moment when a subhalo enters its orbit around the host halo and starts losing mass, as shown in Fig. 4. The upper diagram is for the subhaloes of M31 while the lower one for the subhaloes of the MW. Only subhaloes which survived until the present time were plotted. The solid line in each panel indicates our completeness limit of 100 particles, corresponding to $M = 2.5 \times 10^7 h^{-1} M_{\odot}$.

ready have the correct masses around $10^8 - 10^9 M_{\odot}$ and not enough time to evolve anymore. If they are also dwarf spheroidals today they would need to be dwarf spheroidals already at the moment of orbit entry. A process which could lead to the formation of a dwarf spheroidal (or a dwarf elliptical) at large distance from a host galaxy is a collision of its progenitor with another similar object.

Another class of satellites that can be distinguished in Fig. 8 are the galaxies which enter their orbits early and possess low masses of the order of a few times $10^7 M_{\odot}$. They would then evolve by tidal stirring, like normal dwarf spheroidals, leading to similar objects but of much smaller masses. These could be the progenitors of the ultra faint

dwarfs with expected present masses of around $10^6 M_{\odot}$ and smaller. As demonstrated in Klimentowski et al. (2009) the tidal stripping alone does not significantly change the mass-to-light ratios so if they indeed possess high M/L values, they must be due to the processes involving the evolution of the baryonic component, in particular the gas dynamics. Indeed, their very low initial masses could suppress star formation in the early stages (e.g. White & Rees 1978; Kauffmann, White & Guiderdoni 1993; Mayer et al. 2007). Then they would host very few stars from the beginning which explains why they possess so few stars at the present time (Haiman, Rees & Loeb 1997).

Obviously, the mass resolution of the simulation described here is not sufficient to study the tidal stripping of satellites in detail. Figures 3 and 4 should therefore be considered only as indicative that this process is indeed present. In order to make reliable predictions on its effectiveness one needs to follow the evolution of dwarf galaxies with much higher resolution, which usually means evolving a single dwarf in a fixed potential of the host, as done e.g. in Klimentowski et al. (2007, 2009). Our purpose here is rather to investigate other possible scenarios for the formation of early type dwarfs which involve neighbours. The following sections are therefore devoted to the evolution of satellites in groups and the merging of satellites.

4 SATELLITES IN GROUPS

It has been recently proposed that the infall of subhaloes on to a large halo might occur in groups. The claims have been based both on N -body simulations (e.g. Li & Helmi 2008; Angulo et al. 2009) and observational data (e.g. D’Onghia & Lake 2008; Metz et al. 2009a). The distribution of dwarf satellites of the MW also suggests that they did not infall from completely random directions and form a disk-like structure (Metz et al. 2007, 2009a). If such groups of infalling haloes were bound the probabilities of their close interactions and mergers before the infall would be much higher than for randomly distributed haloes. In this case the haloes inside such groups could be the progenitors of at least some dwarf spheroidal or elliptical galaxies forming them either by tidal interactions or collisions. In this section we study such a possibility in detail.

4.1 Group finding algorithm

Our group finding algorithm is a generalized version of the friends-of-friends (FOF) algorithm (Davis et al. 1985). As in the classical FOF procedure, we define a linking length. An additional parameter is the number of simulation outputs or a time period. Two haloes are considered to form a group if they are closer to each other than the linking length l for a given time period p . Each pair of haloes is checked. If one of the haloes which meet the criteria is already a member of a group, then the other one is added. When both haloes are already members of different groups, then the groups are merged. The algorithm reduces to the standard FOF when the period is set to a single snapshot.

The algorithm is capable of finding many different kinds of groups. We have not used all its possibilities though. One of the most important features of the algorithm is the fact

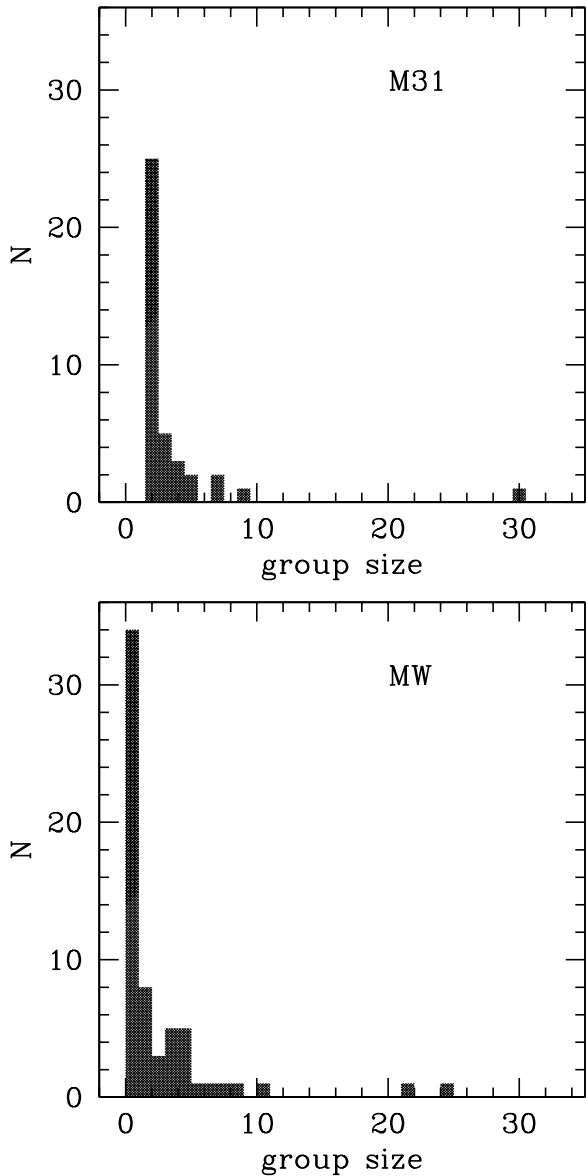


Figure 9. The distribution of group size (measured as number of group members) in M31 (upper panel) and the MW (lower panel). The groups were identified by applying the group finding algorithm with parameters: $l = 100 h^{-1}$ kpc, $p = 1.5$ Gyr, $t_1 = 7$ Gyr, $t_2 = 10.5$ Gyr for M31 and $l = 100 h^{-1}$ kpc, $p = 1.5$ Gyr, $t_1 = 0.2$ Gyr, $t_2 = 13.4$ Gyr for the MW.

that a group does not have to be strictly defined in time. For example, two haloes could form a group at one time, while one of these haloes could form a group with a third halo at a different time. Although we have two different groups of two haloes they are linked together to form one group by a common halo. If we do not want such linking we need to define a time period (with the starting moment t_1 and the ending moment t_2 where $t_2 - t_1 \geq p$), at which we want the algorithm to actually link the haloes. In practice, we use long time periods to find the groups and study their history, and then reapply the algorithm with a short time period at the time of infall to study the group behaviour in its host halo. The set of four parameters l, p, t_1, t_2 completely define

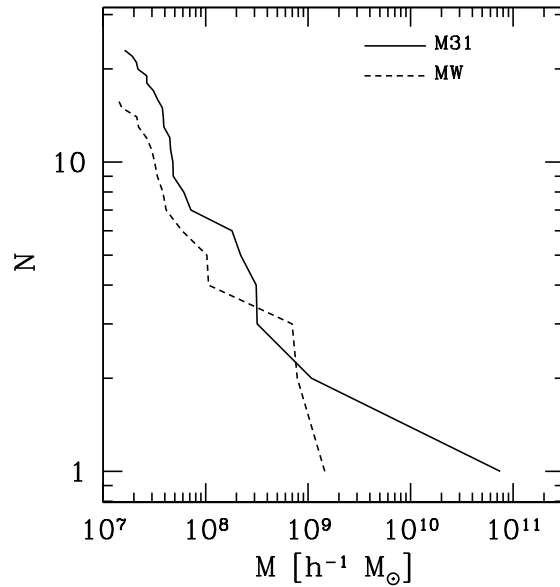


Figure 10. The cumulative mass functions of the largest groups in M31 (LGA, solid line) and the MW (LGM, dashed line).

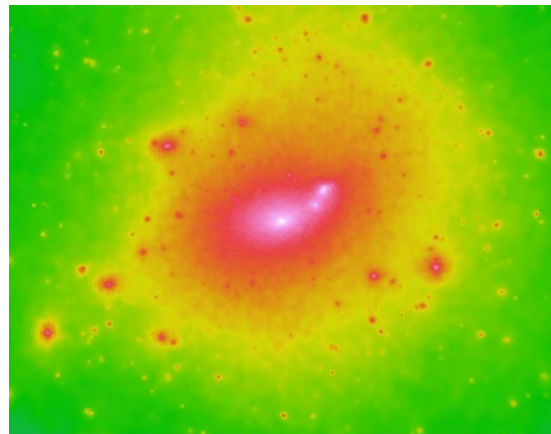


Figure 11. M31 together with its largest subhalo visible to the upper right of the main halo. The size of the image is $200 h^{-1}$ kpc.

the algorithm. Obviously, it can be run on different subsets of haloes. We have run the algorithm for the subhaloes of the two most massive haloes, the M31 and the MW. A subhalo was defined as before as a halo which in at least one simulation output was closer to the host than one virial radius.

4.2 Results of the group finding for M31

We tested different sets of parameters of the algorithm. We were looking for a set of parameters which would recover whole complete groups but would also reject haloes that were members of the group for a short time. Results are quite stable and changing the linking length and the period by less than 30 per cent affects the group membership very little. Finally, two different sets of parameters of the group finder were used. The first run for M31 was made with $l = 100 h^{-1}$

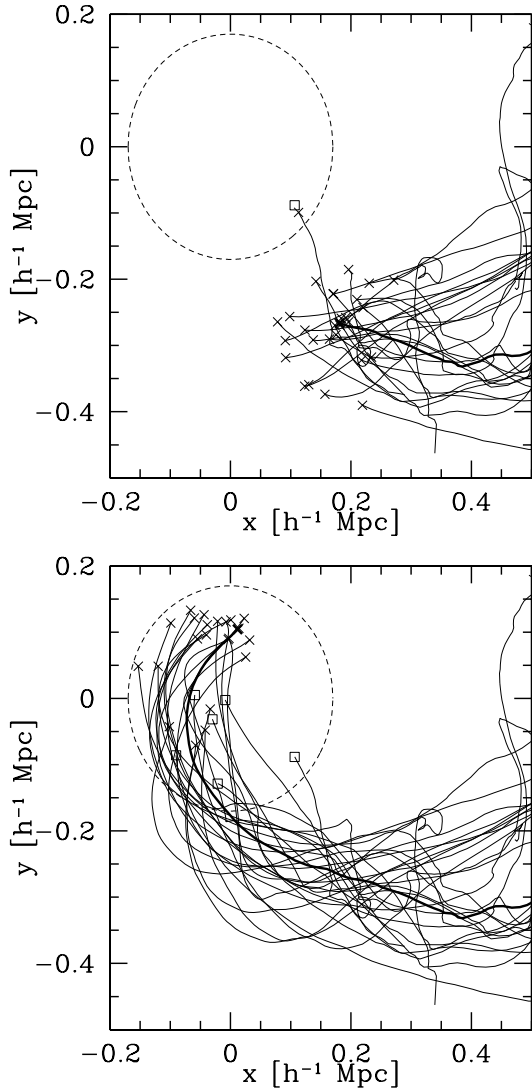


Figure 12. Trajectories of the subhaloes in the Large Group of Andromeda (LGA) starting around 6 Gyr from the beginning of the simulation. The upper panel shows the positions of subhaloes at 9 Gyr, the lower one at present (13.4 Gyr). In both panels the biggest halo is indicated by the thicker line. The dashed circle marks the present virial radius of M31. A square at the end of the line indicates that the halo was destroyed before the end of the simulation, a cross shows the position of a halo which survived until the present.

kpc, $p = 1.5$ Gyr, $t_1 = 0.2$ Gyr, $t_2 = 13.4$ Gyr, thus in this case we look for groups in almost the whole duration of the simulation. The linking length of $100 h^{-1}$ kpc is sufficient for finding large groups of subhaloes.

As a result we get one large group of 116 haloes and about 40 small groups with up to 10 haloes. It turns out that the large group is indeed a bound structure, while the smaller groups are just accidentally linked. The large group was the first target of the analysis. The next step was to narrow down the criteria of the group finder. In the second run we used $l = 100 h^{-1}$ kpc, $p = 1.5$ Gyr, $t_1 = 7$ Gyr, $t_2 = 10.5$ Gyr. The linking length remains the same, but the period at which the linking is made was reduced to the time between 7 and 10.5 Gyr which roughly corresponds to

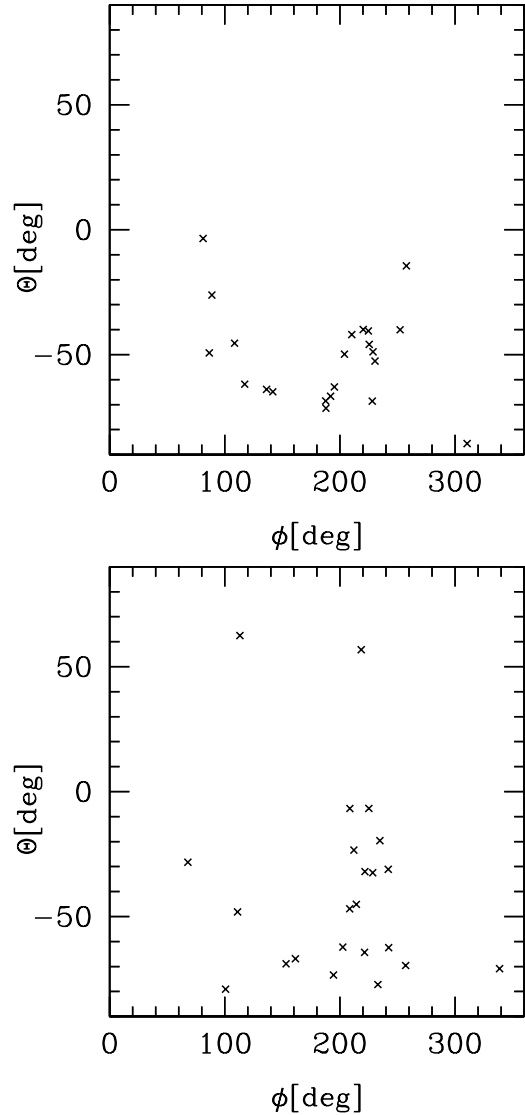


Figure 13. The directions of the angular momentum vectors of LGA subhaloes with respect to M31. The crosses indicate the angular coordinates of the vectors (in the spherical coordinate system) at the time of infall, $t = 9$ Gyr (upper panel) and at the last simulation output $t = 13.4$ Gyr (lower panel). The coordinate system was chosen so that the angular momentum vector of M31 points along the z axis and the orientation of x and y (different in each panel) so that the data points appear centrally in the plots.

the infall time of the large group on to M31. This way we were able to study the large group itself at a time close to its accretion and later. The second run thus can be treated as a filter applied on the first run allowing to reject haloes which deviated from the group before infall. At this point the results are even less influenced by the exact values of the parameters.

4.2.1 The large group of M31

The upper panel of Fig. 9 shows the histogram of the distribution of the group size following from the second run of the group finding algorithm for M31. With the adopted parameters the largest group consists of 30 haloes. From now

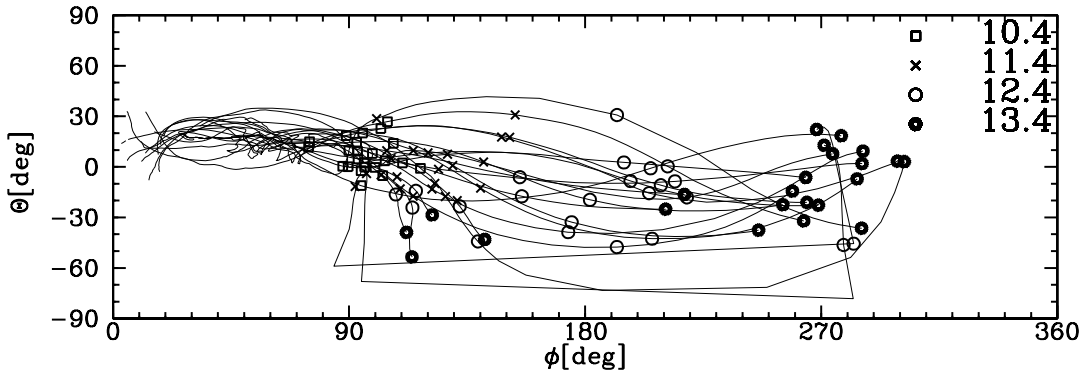


Figure 14. Orbits of the LGA subhaloes as seen by the observer placed at the centre of M31. The spherical coordinate system was oriented so that the angular momentum vector of the host points along the z axis and the orientation of the x and y axis was chosen so that the trajectories are continuous between $\phi = 0$ and 360° . Different symbols correspond to snapshots at different times (in Gyr) indicated in the legend.

on we call it the Large Group of Andromeda (LGA). Few tens of smaller groups are also found. The cumulative mass function of the LGA shown with the solid line in Fig. 10 illustrates its nature. The group consists of one very large halo of mass $M = 7.5 \times 10^{10} h^{-1} M_\odot$, well visible as the largest subhalo in the image of M31 shown in Fig. 11, and several tens of smaller haloes which are actually its satellites. Figure 12 shows the spatial distribution of the haloes in the group at two different times. We did not find any mergers inside such a group.

4.2.2 Observational effects of a LGA-like group

We now consider the present effects of an infall of a LGA-like group in the past. In this case we have a large halo which falls on to M31 along with the set of its satellites. In the simulation the large halo survives until the end, but eventually it will merge with M31. We are more interested in the properties of the satellites. The question is whether we can detect such a past merger by studying only the properties of dwarfs at present.

Figure 13 shows the distribution of the angular momenta vectors of the LGA subhaloes with respect to M31. Only the direction of the vector is shown in the spherical coordinate system. The orientation of the system was chosen so that the z axis points along the total angular momentum of M31. One can clearly see that during the infall (upper panel) angular momenta of the subhaloes are correlated as postulated by Li & Helmi (2008) who defined groups by the separation of angular momenta vectors. In our case however only some of the haloes show this pattern and several others have their angular momentum vectors differing more than the value of only 10° used by Li & Helmi. This suggests that the method of group finding by comparing only angular momentum orientations may miss larger objects or other bound subhaloes. The lower panel of Fig. 13 shows the distribution in the last simulation output, i.e. 4.4 Gyr later. This time period roughly corresponds to half of the group orbit around M31, as can be seen in Fig. 12. During that time the angular momenta were modified and no clear pattern seems to be preserved.

Figure 14 shows the LGA haloes orbits projected on

to the sky. The observer was placed in the M31 centre and the coordinate system was again chosen so that the z axis is aligned with the angular momentum of M31. The haloes are infalling from one well-defined region in the sky but the spread increases with time. It reaches a maximum around 12.4 Gyr when the haloes occupy almost half of the sky. Then the haloes from the main group seem to fall back on the group again, but some other are left in the opposite part of the sky. This example suggests that the alignment of angular momenta of infalling satellites is not well conserved, even though the group has not yet decayed (see also Libeskind et al. 2007). One should thus be very careful when trying to reproduce the histories of dwarf galaxies using their present proper motions. Metz et al. (2007) studied the so-called disk of satellites in the LG. They found that the distribution of MW and M31 satellites is not isotropic, and it rather forms a disk. It has been claimed that this kind of structure could be an effect of a group infall on to the MW halo (Li & Helmi 2008). Based on our result we conclude that such a disk is probably not an effect of a group infall unless it happened very recently.

4.2.3 Smaller groups of M31

The upper panel of Fig. 9 shows that apart from the large group there is a number of smaller groups consisting of usually two, sometimes several haloes. It is interesting to check whether haloes in such groups could strongly interact with each other. We have calculated the escape velocities from such groups and compared them to the true velocities of the haloes. It turns out that for the majority of the groups the subhaloes are only by chance falling on to the host halo from the same direction and are not bound to each other. Several of such groups of two haloes are marginally bound for very short periods of time. We studied in detail mass histories of such cases and concluded that no significant mass transfer is present. These haloes are not massive enough to influence their neighbourhood by tidal interactions and to stay bound for a longer period of time.

4.3 Results of the group finding for MW

The same algorithm was applied to the MW subhaloes. The analysis shows that there are no groups similar to the LGA. The lower panel of Fig. 9 shows the distribution of group sizes obtained with $l = 100 h^{-1}$ kpc, $p = 1.5$ Gyr, $t_1 = 0.2$ Gyr, $t_2 = 13.4$ Gyr. We get a few tens of smaller groups and a larger one consisting of 23 subhaloes, which we will call the Large Group of MW or LGM (with these parameters LGA had 116 members). A closer inspection shows that this group, although of different nature than LGA, is an interesting object by itself. Figure 10 presents the cumulative mass function of this group with the dashed line. The group consists of four larger subhaloes with masses around $M = 10^9 h^{-1} M_\odot$ and some smaller ones. Thus, in contrast to LGA, this is a group of satellites of comparable size, rather than a single large halo with its subhaloes. Unfortunately the infall time of the group is very late, it starts at around 12 Gyr from the beginning of the simulation and is not completed by the end. This prevents us from studying the future evolution of such a group inside the MW halo.

The group was formed around 4 Gyr from the beginning of the simulation. During most of the time it consists of 12 haloes, while the rest is accreted late, when the group falls on to the MW. A careful analysis shows that there is no significant mass transfer between large members. The smaller subhaloes tend to lose mass but this process is much slower than for MW subhaloes and in total it does not amount to more than a few per cent of the initial mass. The larger subhaloes tend to gain mass both from smaller satellites and from other infalling objects, but this process again is very slow and insignificant. We conclude that the group members do not undergo any significant evolution inside the group.

5 MERGERS AND INTERACTIONS OF THE HALOES

In the previous section we have shown that being a member of a group of subhaloes does not significantly affect the evolution of a given subhalo and thus cannot by itself lead to the formation of an early type galaxy. Another possible channel by which such objects could form are interactions and direct mergers of subhaloes. This issues have already been addressed to some extent by Knebe, Gill & Gibson (2004) and Knebe et al. (2006) where they found that on average 30 per cent of the substructure population experienced encounters and that such interactions can account for a significant fraction of mass loss. In this section we address the question of how often such mergers and interactions occur and whether they can indeed lead to the formation of dwarf spheroidals and ellipticals.

5.1 Algorithm for finding interacting haloes

The algorithm presented here was based on finding and selecting interacting haloes. We look for haloes between which particles are exchanged. For each halo an interaction is defined by the following pair of parameters: the mass of all the other haloes taking part in the encounter expressed as a fraction of the studied halo's mass, m_1 , and the mass fraction gained by the studied halo during the encounter, m_2 .

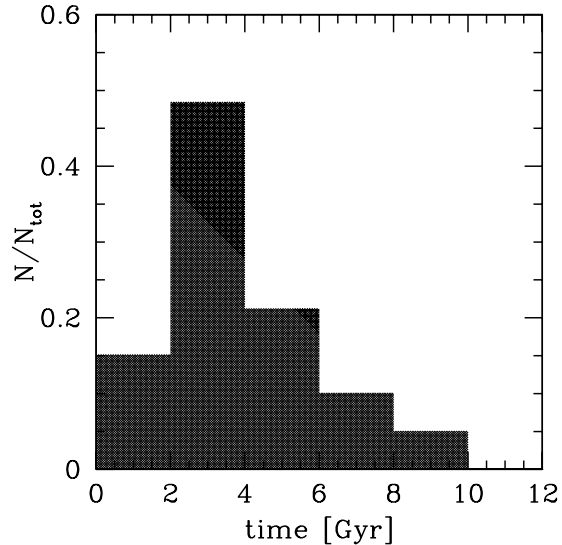


Figure 15. The distribution of interactions for the MW and M31 surviving subhaloes in time for the parameters $m_1 = 0.1, m_2 = 0.3$. The number of interactions was expressed as a fraction of all interactions and the histogram was normalized to unity.

For example, the values $m_1 = 0.5, m_2 = 0.3$ mean that a minimal interaction would be with haloes of mass equal to half the mass of the studied halo from which it gains 30 per cent. For an interaction to be interesting, m_1 has to be large enough, while m_2 needs to be some significant fraction of mass of the other haloes. It is worth noting that a halo might become a subhalo of a larger halo, but then leave it again (as found in cosmological simulations by e.g. Gill et al. 2005; Warnick, Knebe & Power 2008; Ludlow et al. 2009). In such a case the algorithm is capable of finding the interaction for both haloes even though it is not a classical merger. The results will depend on the assumed parameters and the amount of matter exchanged.

The motivation of this approach is the following. In most studies only major mergers are considered. However here we are interested in the probability for a halo to potentially form a dwarf spheroidal or elliptical galaxy by an interaction. Usually, a strong interaction between two haloes would eventually lead to a merger anyway. But the merger itself could happen between haloes which have already exchanged large amounts of mass in past interactions. The resulting merger could seem not to be significant. Our approach allows us to detect each of those interactions and find the strongest one instead of studying only the merger itself. We would like to know what was the magnitude of the strongest of these interactions, as this one had the largest chance to transform the galaxy.

5.2 Interactions of the infalling haloes

We consider only the interactions occurring for those haloes which are still on their way to the host and have not yet become satellites. In this analysis we include only those haloes of the MW and M31 which survived until the end of the simulation with 100 particles or more, as only those are massive enough to be interesting from the observational point of view. We check all detected events so a given surviving sub-

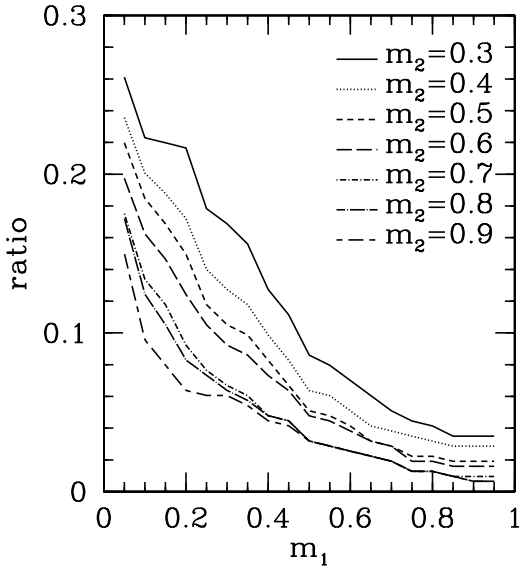


Figure 16. The dependence of the number of interactions on parameters m_1 and m_2 . The lines show the number of events that happened to the surviving sample of 198 M31 and 136 MW subhaloes as a function of m_1 . The different line types correspond to different values of m_2 as indicated by the legend. The numbers give the ratio of the number of interactions to the total number of subhaloes.

halo could have had more than one interaction in the past. We also require that at the moment of interaction the studied halo needs to have at least 50 particles to avoid numerical noise.

As already mentioned, at the end of the simulation M31 has 198 and the MW 136 surviving subhaloes of mass $M > 2.5 \times 10^7 h^{-1} M_\odot$. For example, if we assume that the set of parameters $m_1 = 0.5, m_2 = 0.3$ would be characteristic for a major interaction and apply it, then the algorithm detects a total number of 28 interactions for both M31 and MW subhaloes. This means that less than 10 percent of surviving satellites had a major interaction in the past. This is a significant number, but not high enough to explain the origin of all dwarf spheroidal or elliptical satellites. Figure 15 shows a combined distribution of both M31 and MW interactions in time. Most of the mergers occurred quite early, around redshift $z = 2$ corresponding to 3 Gyr since beginning of the simulation. Such a collision would not have to produce an early type dwarf galaxy immediately, since it would still have a lot of time to evolve in the tidal field of its host.

Note that the shape of the distribution shown in Fig. 15 does not depend strongly on the assumed parameters m_1 and m_2 ; the interactions still occur rather early if we vary those parameters. The total number of interactions detected depends however on these parameters. Figure 16 presents the results of exploring the parameter space in terms of the fraction of subhaloes that experienced interaction (or a number of interactions per subhalo) with a given m_1 and m_2 . As expected, minor interactions are more numerous and the fraction of affected subhaloes decreases strongly with growing m_1 and m_2 .

It turns out that a significant fraction (15-25 percent,

taking the smallest m_1 and the whole range of m_2 in Fig. 16) of subhaloes had some kind of interaction in the past, but only several percent had a strong interaction that could be called a major merger. This suggests that the mergers, while present in the histories of some dwarf galaxies, could not explain the large numbers of spheroidals and ellipticals in the LG. Still, majority of dwarf galaxies did not have even a slight interaction with another dwarf in the past.

However, this result depends on the assumption that we count the interactions only when the halo has at least 50 particles, corresponding to the mass of $M = 1.25 \times 10^7 h^{-1} M_\odot$, which we find to be the lowest limit at which this study still makes sense. We have verified that the assumed threshold of 50 particles for the algorithm is rather realistic: with increasing threshold the numbers of interactions decrease very slowly, while lowering the threshold would produce many more interactions. This could be easily understood: according to Fig. 15 most of the encounters are expected to happen early when the haloes are in general less massive. Interactions with low particle numbers may however be affected by numerical noise and therefore their statistics is not reliable.

6 DISCUSSION

We have analyzed a constrained simulation of the local Universe which reproduces the main properties of the LG. The simulation outputs were used to study the population of subhaloes around the largest galaxies. Our attention was focused on those signatures of the evolution that can shed some light on the possible scenarios of the formation of early type dwarf galaxies, dwarf ellipticals and dwarf spheroidals, that we presently observe. Assuming that the progenitors of these objects are baryonic disks embedded in dark matter haloes, some mechanisms are required that could transform the disks into bulges. In the case of purely gravitational interactions, such an evolution can occur by three channels: the tidal stirring in the gravitational field of the host galaxy, interaction of small haloes infalling together in groups and mergers between prospective subhaloes.

A quantitative study of the effect of tidal forces on a single subhalo usually requires a different simulation setup and much higher resolution (e.g. Klimentowski et al. 2007, 2009). In the present context the tidal stripping manifests itself in the statistical properties of our subhalo population. We found that the mass function of satellites evolves significantly between $z = 1$ and $z = 0$ so that the number of small subhaloes increases and the number of larger ones decreases, as expected if subhaloes lose mass by tides. On average, the mass of satellites at the end of the simulation is smaller than at the moment of their infall on to the halo of their host. For most subhaloes the transition from the phase of mass accretion to the phase of mass loss can be easily identified and corresponds to the moment of entry into the host halo. We find that this maximum mass or entrance moment can occur at a wide range of redshifts but typically more massive subhaloes enter the vicinity of their hosts earlier, around $z = 1$ and before (see also Diemand et al. 2007). This distribution in redshift suggests that those massive subhaloes could be the progenitors of present-day dwarf spheroidals since they have still a lot of time to evolve. The less massive subhaloes entering later could still be dwarf irregulars today on one

of their first passages around the MW like the Magellanic Clouds (Besla et al. 2007).

We also studied the evolution of satellites in groups. Although many groups were identified both around M31 and the MW, they are usually loosely bound and their member subhaloes do not strongly interact with each other. Therefore we conclude that being a member of a group cannot result in any morphological transformation of a dwarf galaxy. Membership in a group could however explain some particular distributions of satellites around big galaxies, provided that the group infall occurred recently. Using a large group identified in the vicinity of our simulated M31 we have demonstrated that the group forms a coherent structure at infall but dissipates on a rather short timescale.

Mergers between subhaloes offer another possibility for the formation of early type dwarfs. We found that around 10 percent of present-day subhaloes of M31 and the MW underwent a major interaction with another halo in the past. Most of the events took place early on, around 7 – 11 Gyr ago, when the objects have not yet become satellites of big galaxies. This suggests that dwarf ellipticals could be a product of mergers rather than tidal evolution, as they tend to be more isolated objects found further from the MW than dwarf spheroidals.

ACKNOWLEDGMENTS

The simulations used in this work were performed at the Leibniz Rechenzentrum Munich (LRZ) and at the Barcelona Supercomputing Centre (BSC), partly funded by the DEISA Extreme Computing Project (DECI) SIMU-LU. JK and EL acknowledge support by the Polish Ministry of Science and Higher Education under grant NN203025333 as well as by the Polish-German exchange program of Deutsche Forschungsgemeinschaft. AK is supported by the MICINN through the Ramon y Cajal programme. SG acknowledges a Schonbrunn Fellowship at the Hebrew University Jerusalem. LAMV acknowledges financial support from Comunidad de Madrid through a PhD fellowship. GY is supported by the Spanish Ministry of Education through research grants FPA2006-01105 and AYA2006-15492-C03. YH has been partially supported by the ISF (13/08). We are grateful for the hospitality of the Astrophysikalisches Institut Potsdam where part of this work was done. We acknowledge the LEA Astro-PF collaboration and the ASTROSIM network of the European Science Foundation (Science Meeting 2387) for the financial support of the workshop ‘The local Universe: from dwarf galaxies to galaxy clusters’ held in Jabłonna near Warsaw in June/July 2009, where this work was completed.

REFERENCES

- Angulo R. E., Lacey C. G., Baugh C. M., Frenk C. S., 2009, *MNRAS*, 399, 983
- Belokurov V., Walker M. G., Evans N. W. et al., 2008, *ApJ*, 686, L38
- Besla G., Kallivayalil N., Hernquist L., Robertson B., Cox T., van der Marel R., Alcock C., 2007, *ApJ*, 668, 949
- Bullock J. S., Johnston K. V., 2005, *ApJ*, 635, 931
- Davis M., Efstathiou G., Frenk C., White S., 1985, *ApJ*, 292, 371
- Diemand J., Kuhlen M., Madau P., 2007, *ApJ*, 667, 859
- D’Onghia E., Lake G., 2008, *ApJ*, 686, L61
- Fouqué P., Solanes J. M., Sanchis T., Balkowski C., 2001, *A&A*, 375, 770
- Gill S. P. D., Knebe A., Gibson B. K., 2004a, *MNRAS*, 351, 399
- Gill S. P. D., Knebe A., Gibson B. K., Dopita M. A., 2004b, *MNRAS*, 351, 410
- Gill S. P. D., Knebe A., Gibson B. K., 2005, *MNRAS*, 356, 1327
- Giocoli C., Tormen G., van den Bosch F. C., 2008, *MNRAS*, 386, 2135
- Haiman Z., Rees M., Loeb A., 1997, *ApJ*, 476, 458
- Hayashi E., Navarro J. F., Taylor J. E., Stadel J., Quinn T., 2003, *ApJ*, 584, 541
- Hoffman Y., Ribak E., 1991, *ApJ*, 280, L5
- Hudson M. J., 1993, *MNRAS*, 265, 43
- Kampakoglou M., Benson A. J., 2007, *MNRAS*, 374, 775
- Karachentsev I. D., Karachentseva V. E., Huchtmeier W. K., Makarov D. I., 2004, *AJ*, 127, 2031
- Kauffmann G., White S., Guiderdoni B., 1993, *MNRAS*, 264, 201
- Kazantzidis S., Mayer L., Mastropietro C., Diemand J., Stadel J., Moore B., 2004a, *ApJ*, 608, 663
- Kazantzidis S., Moore B., Mayer L., 2004b, in Prada F., Martinez Delgado D., Mahoney T. J., eds, *Satellites and Tidal Streams*, ASP Conference Series, Vol. 327, p. 155
- Karachentsev I. D., Karachentseva V. E., Huchtmeier W. K., Makarov D. I., 2004, *AJ*, 127, 2013
- Klimentowski J., Lokas E. L., Kazantzidis S., Prada F., Mayer L., Mamon G. A., 2007, *MNRAS*, 378, 353
- Klimentowski J., Lokas E. L., Kazantzidis S., Mayer L., Mamon G. A., 2009, *MNRAS*, 397, 2015
- Klypin A., Kravtsov A. V., Bullock J. S., Primack J. R., 2001, *ApJ*, 554, 903
- Klypin A., Hoffman Y., Kravtsov A. V., Gottlöber S., 2003, *ApJ*, 596, 19
- Knebe A., Gill S. P. D., Gibson B. K., 2004, *PASA*, 21, 216
- Knebe A., Power C., Gill S. P. D., Gibson B. K., 2006, *MNRAS*, 368, 741
- Knollmann S., Knebe A., 2009, *ApJS*, 182, 608
- Kravtsov A. V., Gnedin O. Y., Klypin A. A., 2004, *ApJ*, 609, 482
- Kravtsov A. V., Klypin A., Hoffman Y., 2002, *ApJ*, 571, 563
- Li Y., Helmi A., 2008, *MNRAS*, 385, 1365
- Libeskind N. I., Frenk C. S., Cole S., Helly J. C., Jenkins A., Navarro J. F., Power C., 2005, *MNRAS*, 363, 146
- Libeskind N. I., Cole S., Frenk C. S., Okamoto T., Jenkins A., 2007, *MNRAS*, 374, 16
- Libeskind N. I., Yepes G., Knebe A., Gottlöber S., Hoffman Y., Knollmann S. R., 2009, *MNRAS*, submitted
- Lokas E. L., 2009, *MNRAS*, 394, L102
- Lokas E. L., Hoffman Y., 2001, in Spooner N. J. C., Kudryavtsev V., eds, *Proc. 3rd International Workshop, The Identification of Dark Matter*. World Scientific, Singapore, p. 121
- Lokas E. L., Klimentowski J., Kazantzidis S., Mayer L., 2008, *MNRAS*, 390, 625
- Ludlow A. D., Navarro J. F., Springel V., Jenkins A., Frenk C. S., Helmi A., 2009, *ApJ*, 692, L931
- Mateo M., 1998, *ARA&A*, 36, 435
- Mayer L., Governato F., Colpi M., Moore B., Quinn T., Wadsley J., Stadel J., Lake G., 2001, *ApJ*, 559, 754
- Mayer L., Kazantzidis S., Mastropietro C., Wadsley J., 2007, *Nature*, 445, 738
- Metz M., Kroupa P., Jerjen H., 2007, *MNRAS*, 374, 1125
- Metz M., Kroupa P., Jerjen H., 2009a, *MNRAS*, 394, 2223
- Metz M., Kroupa P., Theis C., Hensler G., Jerjen H., 2009b, *ApJ*, 697, 269
- Peñarrubia J., Navarro J. F., McConnachie A. W., 2008, *ApJ*, 673, 226
- Reiprich T. H., Böhringer H., 2002, *ApJ*, 567, 716
- Sakamoto T., Hasegawa T., 2006, *ApJ*, 653, L29

- Sales L. V., Navarro J., Abadi M. G., Steinmetz M., 2007a, MNRAS, 379, 1475
- Sales L. V., Navarro J., Abadi M. G., Steinmetz M., 2007b, MNRAS, 379, 1464
- Simon J. D., Geha M., 2007, ApJ, 670, 313
- Spergel D. N. et al., 2007, ApJS, 170, 377
- Springel V., 2005, MNRAS 364, 1105
- Springel V., Di Matteo T., Hernquist L., 2005, MNRAS, 361, 776
- Sakamoto T., Hasegawa T., 2006, ApJ 653, L29
- Tikhonov A. V., Klypin A., 2009, MNRAS, 395, 1915
- Tolstoy E., Hill V., Tosi M., 2009, ARA&A, 47, 371
- Tonry J. L., Blakeslee J. P., Ajhar E. A., Dressler A., 2000, ApJ, 530, 625
- Tonry J. L., Dressler A., Blakeslee J. P., Ajhar E. A., Fletcher A. B., Luppino G. A., Metzger M. R., Moore C. B., 2001, ApJ, 546, 681
- van den Bergh S., 1999, A&AR, 9, 273
- van der Marel R. P., Guhathakurta P., 2008, ApJ, 678, 187
- Warnick K., Knebe A., Power C., 2008, MNRAS, 385, 1859
- White S., Rees M., 1978, MNRAS, 183, 341
- Willick J. A., Courteau S., Faber S. M., Burstein D., Dekel A., Strauss M. A., 1997, ApJ, 109, 333
- Zaroubi S., Hoffman Y., Dekel A., 1999, ApJ, 520, 413
- Zucker D. B., Belokurov V., Evans N. W. et al., 2006, ApJ, 650, L41